Diabetic Endothelial Nitric Oxide Synthase Knockout Mice Develop Advanced Diabetic Nephropathy

Takahiko Nakagawa,* Waichi Sato,* Olena Glushakova,* Marcelo Heinig,* Tracy Clarke,† Martha Campbell-Thompson,† Yukio Yuzawa,‡ Mark A. Atkinson,§ Richard J. Johnson,* and Byron Croker§‖

**Division of Nephrology, †Molecular Pathology and Immunology Core Lab, and §Department of Pathology, Immunology and Laboratory Medicine, University of Florida, and ‖Pathology and Laboratory Medicine Service, North Florida/South Georgia Veterans Health System, Gainesville Florida; and ‡Department of Clinical Immunology of Internal Medicine, Nagoya University Graduate School of Medicine, Nagoya, Japan*

The pathogenesis of diabetic nephropathy remains poorly defined, and animal models that represent the human disease have been lacking. It was demonstrated recently that the severe endothelial dysfunction that accompanies a diabetic state may cause an uncoupling of the vascular endothelial growth factor (VEGF)-endothelial nitric oxide (eNO) axis, resulting in increased levels of VEGF and excessive endothelial cell proliferation. It was hypothesized further that VEGF-NO uncoupling could be a major contributory mechanism that leads to diabetic vasculopathy. For testing of this hypothesis, diabetes was induced in eNO synthase knockout mice (eNOS KO) and C57BL6 controls. Diabetic eNOS KO mice developed hypertension, albuminuria, and renal insufficiency with arteriolar hyalinosis, mesangial matrix expansion, mesangiolysis with microaneurysms, and Kimmelstiel-Wilson nodules. Glomerular and peritubular capillaries were increased with endothelial proliferation and VEGF expression. Diabetic eNOS KO mice showed increased mortality at 5 mo. All of the functional and histologic changes were improved with insulin therapy. Inhibition of eNO predisposes mice to classic diabetic nephropathy. The mechanism likely is due to VEGF-NO uncoupling with excessive endothelial cell proliferation coupled with altered autoregulation consequent to the development of preglomerular arteriolar disease. Endothelial dysfunction in human diabetes is common, secondary to effects of glucose, advanced glycation end products, C-reactive protein, uric acid, and oxidants. It was postulated that endothelial dysfunction should predict nephropathy and that correction of the dysfunction may prevent these important complications.

J Am Soc Nephrol 18: 539–550, 2007. doi: 10.1681/ASN.2006050459

Diabetes is an increasingly common condition, with 30 to 40% of affected patients eventually developing nephropathy. Although diabetic nephropathy is epidemic, the pathogenesis is not well defined, in part because of the lack of an animal model that reproduces human disease (1). Diabetic nephropathy is characterized by glomerular hypertrophy, glomerular basement membrane (GBM) thickening, and mesangial expansion in its early stages, which is followed by mesangiolysis, glomerular microaneurysms, or nodular lesions (Kimmelstiel-Wilson nodule) as the lesion advances (2,3). The prevalence and clustering of mesangiolysis (36%), Kimmelstiel-Wilson nodules (39%), and glomerular microaneurysms (12%) has led to the hypothesis that they are pathogenically interrelated (2,3). Although several animal models have been shown to develop early stages of diabetic nephropathy, to our knowledge, a rodent model that demonstrates the advanced stage of diabetic nephropathy has yet to be described (1). In addition to the aforementioned histologic changes, abnormal angiogenesis has been observed in human diabetic nephropathy and has been linked with disease progression (4). Recently, new vessel formation was demonstrated at the vascular pole of the glomerulus in human diabetic kidney, and the presence of these extra vessels correlated with increased vascular endothelial growth factor (VEGF) expression (5). VEGF also mediates renal hypertrophy, an increase in GFR, and urinary protein excretion in early experimental diabetic nephropathy (6,7), suggesting a potentially deleterious role of VEGF in diabetic renal disease.

VEGF is the major angiogenic cytokine that stimulates endothelial cell proliferation and migration. VEGF action depends primarily on endothelial nitric oxide (eNO) production (8). Hence, coupling of VEGF with eNO could be important in maintaining endothelial integrity in vessels. However, the role of VEGF is complicated in the diseased kidney. VEGF is renoprotective in both acute and chronic nondiabetic renal disease (9) in contrast to diabetic nephropathy. Indeed, VEGF administration in the renal ablation model was found to stimulate capillary repair and improve renal function (9).

Received May 11, 2006. Accepted October 31, 2006.

Published online ahead of print. Publication date available at www.jasn.org.

Address correspondence to: Dr. Takahiko Nakagawa, Division of Nephrology, Hypertension and Transplantation, University of Florida, PO Box 100224, Gainesville, FL 32610-0224. Phone: 352-392-2448; Fax: 352-392-5465; E-mail; nakagt@medicine.ufl.edu

ISSN: 1046-6673/1802-0539

One potential explanation for the paradox of VEGF and kidney disease might be accounted for by the bioavailability of eNO, which is severely reduced in diabetes (10,11). Given the increased expression of VEGF in diabetes, the reduced NO bioavailability theoretically could result in an uncoupling of VEGF with NO. It is interesting that there is evidence that blockade of eNO results in a compensatory increase in VEGF (12), which engages an NO-independent pathway to stimulate endothelial cell proliferation (13). This may result in deleterious as opposed to beneficial effects of VEGF (14–17). Indeed, other groups and ours have shown that long-term inhibition of NO synthase (NOS) resulted in severe vascular disease along with *de novo* VEGF expression in renal vessels as well as in coronary arteries, where endothelial proliferation, monocyte infiltration, and vascular smooth muscle cell proliferation were prominent (18,19).

We hypothesized that an uncoupling of VEGF with eNO might contribute to the vascular complications that are observed in diabetes. Indeed, we were able to demonstrate that uncoupling of VEGF with eNO could stimulate an excessive endothelial cell proliferation under high glucose conditions (20). To test our hypothesis in an *in vivo* model of diabetes, we used eNOS KO mice, which are incapable of endogenously producing endothelial cell NO. We performed experiments to determine whether diabetic mice that lack eNOS might be predisposed to diabetic nephropathy.

Materials and Methods

Experimental Animals

Experiments were performed following a protocol that was approval by the Animal Care and Use Committee of the University of Florida . C57Bl/6J mice (C57BL6) and C57BL/6J-Nos3tm1Unc (eNOS KO mice; Jackson Laboratory, Bar Harbor, ME) that were aged 8 wk were rendered diabetic with intraperitoneal injections of streptozotocin (100 mg/kg per d for 2 consecutive days) that was freshly dissolved in 0.01 M citrate buffer (pH 4.5). Development of diabetes (defined by blood glucose >250 mg/dl) was verified 1 wk after the first streptozotocin injection. For blood sugar control, a single insulin pellet (Linshin Canada, Ontario, Canada) was implanted subcutaneously for 5 mo. Blood glucose was monitored every 2 wk, and when the fasting blood glucose was >200 mg/dl, an additional insulin pellet was inserted. A total of six groups were examined with 10 mice for each group at starting points. Nondiabetic, diabetic, and diabetic mice (C57BL6 and eNOS KO) with insulin treatment were examined. Systolic BP was assessed as the mean value of five to 10 consecutive measurements that were obtained in the morning using a tail-cuff sphygmomanometer (Visitech BP2000; Visitech Systems, Apex, NC). Blood urea nitrogen (BUN) was measured by BUN assay (Diagnostic Chemicals Ltd., Oxford, CT). Urine in bladder was obtained for urinary albumin excretion when the mice were killed. Albumin-to-creatinine ratio was measured with Albuwell M (Exocell, Philadelphia, PA) and Liquid Creatinine Assay (Bioquant, San Diego, CA), respectively.

Renal Histology

Kidneys were fixed in Fekete's fixative (mixture of ethanol, distilled water, 37% formalin, and glacial acetic acid) and embedded in paraffin. Two-micrometer sections were stained with the periodic acid-Schiff reagent (PAS) or the periodic acid-methenamine silver and counterstained with hematoxylin. Indirect immunoperoxidase staining was performed using antibodies to the endothelial antigen thrombomodulin (21) or CD34 (BD Pharmingen, San Jose, CA) (22), to vascular smooth muscle cells with anti–α-smooth muscle actin (Abcam, Cambridge, MA), to fibrin deposition with a polyclonal rabbit anti-mouse fibrin antibody (Innovative Research, Hilltop, Southfield, MI), and to collagen IV deposition with a polyclonal rabbit anti-mouse collagen IV antibody (Chemicon International, Temecula, CA). To detect endothelial cell proliferation, we performed double immunostaining with an antibody to the proliferating cell nuclear antigen Ki-67 (Abcam, Cambridge, MA) and thrombomodulin/CD34. Color was developed using diaminobenzidine as a chromogen. In double staining, Bjoran Purple (BioCare Medical, Concord, CA) was used for thrombomodulin/CD34.

For electron microscopy, kidneys were fixed in 10% formalin fixative, embedded in epoxy resin, and stained with uranyl acetate and lead citrate. GBM measurements and digital images were made using an Advanced Microscopy Techniques (Danvers, MA) digital camera system and measuring package on a Philips (Eindhoven, Netherlands) electron microscope. The thickness of the GBM was estimated by determination of the harmonic mean of a series of orthogonal intercept measurements (23). At least 30 different segments of GBM per mouse from three mice were measured in each treatment group.

Quantification of Morphology

All quantifications were performed in a blinded manner. Using coronal sections of the kidney, all glomeruli (100 to 200 glomeruli) were examined for evaluation of mesangiolysis and nodular lesions. For glomerular mesangial expansion, 30 consecutive glomeruli per animal were examined. The extent of the mesangial matrix (defined as mesangial area) was determined by assessment of the PAS-positive and nucleus-free area in the mesangium. The glomerular area was traced along the outline of the capillary loop using AxioVision image analyzer (Carl Zeiss, Thornwood, NY). Because the ratio of mesangial/glomerular area in nondiabetic C57BL6 is 0.20 ± 0.04 in this study, mesangial expansion is defined with the ratio of mesangial/glomerular area >0.25, which is compatible with a previous report (24). The percentage of glomerular injury was calculated as the number of injured glomeruli divided by that of total glomeruli. Arteriolar morphology was assessed by α-smooth muscle actin staining (25). GBM thickness also was measured at super high magnification (×5200) in light microscopy using Axioplan2 imaging system (Carl Zeiss) with digital imaging software.

Real-Time PCR

To quantify mRNA expression for VEGF-A, we performed real time PCR as described previously (26). The sizes of amplicons were 111 bp (mouse VEGF-A) (27), which includes isoform 167 and 188.

Statistical Analyses

One-way ANOVA followed by Bonferroni was used to compare more than two groups. For comparison between two groups, the unpaired two-tailed *t* test was performed. All tests were performed using the software program inStat (version 3.06; GraphPad, San Diego, CA). Significance was defined as $P < 0.05$.

Results

General Parameters

The induction of type 1 diabetes by streptozotocin resulted in equivalent hyperglycemia in C57BL6 and eNOS KO mice when measured at 3 and 5 mo, as shown in Table 1. However, loss of body weight was more severe in diabetic eNOS KO mice compared with diabetic C57BL6 mice. Systolic BP was higher in nondiabetic eNOS KO mice at 3 mo but fell to lower levels than that in C57BL6 controls at 5 mo. Indeed, BP was unmeasurable in two

Table 1. General characteristics of control and diabetic mice[a]

Characteristic	C57BL6			eNOS KO		
	Non-DM	DM	DM-Ins	Non-DM	DM	DM-Ins
3 mo after diabetes induction						
body weight (g)	30.2 ± 3.1	23.8 ± 1.6[b,c]	26.7 ± 1.4	28.9 ± 1.1	19.4 ± 1.7[b,c]	26.6 ± 2.2
blood glucose (mg/dl)	127 ± 23	379 ± 107[b,c]	144 ± 38	107 ± 20	385 ± 105[b,c]	90 ± 40
SBP (mmHg)	121 ± 7	138 ± 12[b,d]	128 ± 7	136 ± 8[e]	161 ± 13[b,c]	138 ± 14
kidney weight/body weight ($\times 10^{-3}$)	5.0 ± 0.4	6.2 ± 2.7	5.0 ± 0.6	4.7 ± 0.5[f]	8.3 ± 1.2[b,c]	4.8 ± 0.7
urine albumin/creatinine ($\times 10^{-1}$)	1.4 ± 1.3	6.2 ± 4.5[b,c]	0.6 ± 0.5	1.2 ± 0.4	6.1 ± 3.0[b,c]	2.2 ± 0.7
BUN (mg/dl)	12.2 ± 3.0	14.5 ± 2.0	12.0 ± 2.3	14.1 ± 2.5	21.8 ± 6.2[g,h]	17.1 ± 3.0
5 mo after diabetes induction						
body weight (g)	32.0 ± 2.0	23.1 ± 1.8[b,c]	27.4 ± 2.1	29.2 ± 2.1	18.8 ± 3.2[b,c]	25.4 ± 1.4
blood glucose (mg/dl)	137 ± 5	392 ± 30[b,c]	178 ± 30	143 ± 18	392 ± 72[b,c]	180 ± 29
SBP (mmHg)	119 ± 8	132 ± 16[b,c]	119 ± 7	139 ± 11[e]	(124 ± 30) Unmeasurable from 2 mice	148 ± 7
kidney weight/body weight ($\times 10^{-3}$)	5.4 ± 0.3	9.1 ± 1.2[b,c]	5.4 ± 0.5	4.5 ± 0.5	9.0 ± 1.6[b,c]	5.4 ± 0.7
urine albumin/creatinine ($\times 10^{-1}$)	2.5 ± 0.8	5.6 ± 2.3[b]	4.0 ± 1.4	27.0 ± 9.6[f]	107.9 ± 53.2[b,c]	11.6 ± 8.7
BUN (mg/dl)	16.2 ± 2.4	18.5 ± 2.5[b]	15.7 ± 2.2	19.6 ± 1.4[e]	34.8 ± 5.6[b,c]	24.9 ± 3.0[e]

[a]BUN, blood urea nitrogen; Ins; insulin treatment; eNOS KO, endothelial nitric oxide knockout; non-DM, nondiabetic; SBP; systolic BP.
[b]$P < 0.01$ *versus* non-DM.
[c]$P < 0.01$ *versus* DMIns.
[d]$P < 0.05$ *versus* DMIns.
[e]$P < 0.05$ *versus* non-DM C57BL6.
[f]$P < 0.05$ *versus* non-DM C57BL6.
[g]$P < 0.05$ *versus* non-DM.
[h]$P < 0.05$ *versus* DMIns.

of six diabetic eNOS KO mice at 5 mo, whereas two other diabetic eNOS KO mice demonstrated low BP of 92 and 104 mmHg, respectively. Survival of diabetic eNOS KO mice also was lower at 5 mo compared with diabetic C57BL6 mice (Figure 1).

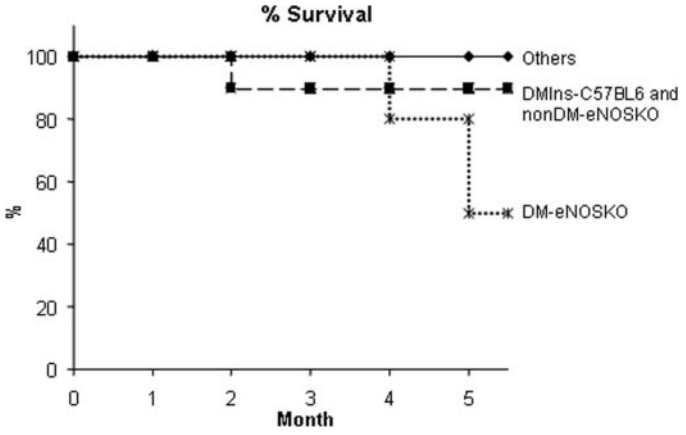

Figure 1. Survival rate of diabetic endothelial nitric oxide synthase knockout (DM eNOS KO) mice at 5 mo. DMIns, diabetes with insulin treatment; NonDM, nondiabetic.

Insulin treatment was associated with significant improvements in blood glucose levels in both C57BL6 and eNOS KO mice. It is interesting that insulin treatment significantly improved blood sugar, BP, and survival in eNOS KO mice (Table 1, Figure 1). Elevated BP at 3 mo was improved with insulin treatment in eNOS KO mice.

Renal Function and Gross Morphology

Diabetes-induced renal hypertrophy was more pronounced in eNOS KO mice (Table 1). Diabetic C57BL6 and eNOS KO mice exhibited higher urinary albumin excretion as well as high BUN levels at 3 mo. However, urinary albumin excretion and BUN levels were higher in eNOS KO mice compared with diabetic C57BL6 mice at 5 mo (Table 1). The administration of insulin at dosages that resulted in normalization of blood sugar prevented the development of renal hypertrophy, proteinuria, and renal dysfunction in both the C57BL6 and the eNOS KO mice (Table 1).

Glomerular Histology

Both C57BL6 and eNOS KO diabetic mice developed mesangial expansion, but it was more prominent in the eNOS KO

mice (Figure 2, A and B; Table 2). As shown in Figure 3, blood glucose levels correlated with mesangial expansion in both C57BL6 mice and eNOS KO mice. It is interesting that glomeruli in eNOS KO were more susceptible to blood glucose than C57BL6 mice in terms of development of mesangial expansion (Figure 3A). Mesangial expansion was associated with collagen IV deposition in diabetic eNOS KO mice (Figures 3C and 4, A through C). Most important, at 3 mo, there were striking findings in diabetic eNOS KO mice, in which mesangiolysis (Figure 2D) and glomerular microaneurysms (Figure 2E) developed. Furthermore, Kimmelstiel-Wilson–like nodular lesions were observed in occasional glomeruli at both 3 and 5 mo. It is interesting that these nodular lesions were composed of nodular mesangial expansion (Figure 2F), acellular PAS-positive

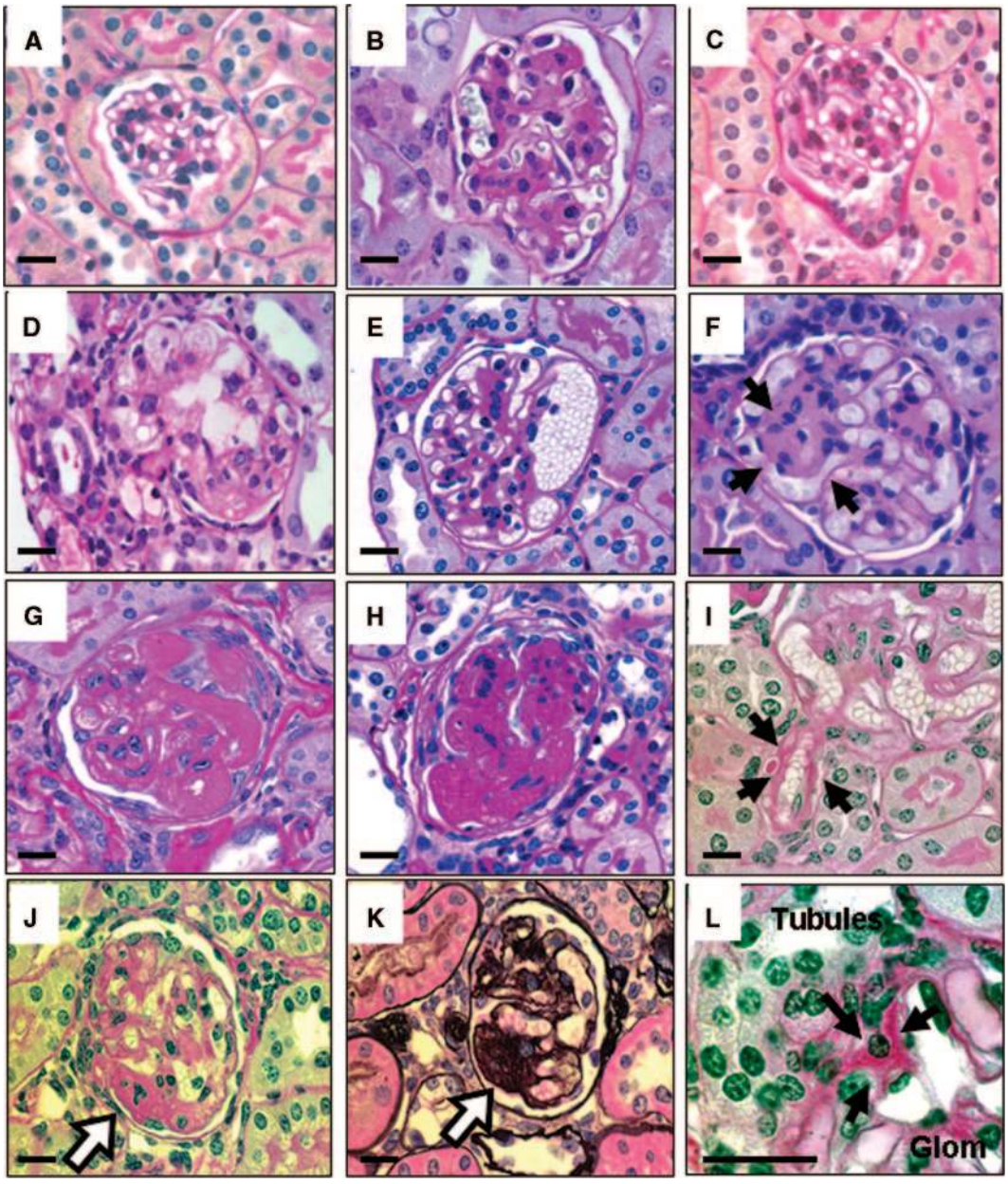

Figure 2. Histology in glomeruli from C57BL6 and eNOS KO mice. (A) Glomerulus in non-DM C57BL6 mouse at 3 mo. (B) DM C57BL6 mouse at 3 mo. (C) Non-DM eNOS KO mouse at 3 mo. (D) DM eNOS KO mouse at 3 mo. Mesangiolysis can be observed in glomerulus. (E) Glomerular microaneurysm in DM eNOS KO mouse at 3 mo. (F) Nodular glomerular expansion in DM eNOS KO mouse at 5 mo. (G) Nodular lesion with acellular periodic acid-Schiff (PAS)-positive material in DM eNOS KO mouse at 3 mo. (H) Diffuse glomerulosclerosis in DM eNOS KO mouse at 3 mo. (I) Arteriolar hyalinosis (arrow) associated with glomerular mesangiolysis in DM eNOS KO mouse at 5 mo. (J) Nodular glomerulosclerosis (arrow) in DM eNOS KO mouse at 5 mo. (K) Nodular glomerulosclerosis on periodic acid-methenamine silver staining in serious section of J in DM eNOS KO mouse at 5 mo. (L) Hyalinosis (arrow) at vascular pole of glomerulus in DM eNOS KO mouse at 5 mo. Bar = 10 μm. Magnifications: ×1000 in A through K; ×2000 in L.

Table 2. Glomeruli with mesangial expansion

Parameter	3 Mo (%)			5 Mo (%)		
	Non-DM	DM	DMIns	Control	DM	DMIns
C57BL6	0.5 ± 0.4	12.6 ± 1.8	3.6 ± 1.3	1.5 ± 0.6	32.0 ± 5.5	12.0 ± 4.5
eNOS KO	5.3 ± 0.6	20.1 ± 5.1[b]	7.3 ± 1.4	5.9 ± 2.8	55.0 ± 9.8[a]	20.0 ± 4.5

[a] $P < 0.01$ *versus* C57BL6-DM at 5 mo.
[b] $P < 0.05$ *versus* non-DM, DMIns at 3 mo.

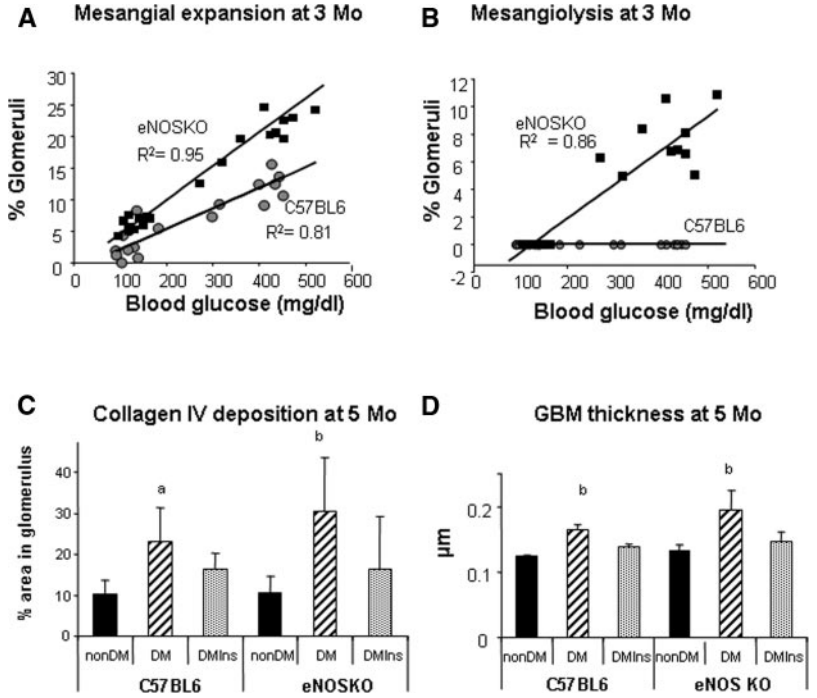

Figure 3. Quantification of histologic analysis. Correlation between blood glucose and mesangial expansion (A) and mesangiolysis (B) at 3 mo. (C) Percentage of positive area for collagen IV deposition in glomerulus. (D) Thickness of glomerular basement membrane (GBM) at 5 mo.

material (Figure 2G), and dense fibrillar mesangial matrix (Figure 2H). Nodular glomerulosclerosis was demonstrated by PAS and periodic acid-methenamine silver staining with serial section of glomeruli (Figure 2, J and K). Fibrin deposition also was detected in the nodular lesion (Figure 4, H and I; Table 3). However, staining for IgG and IgM was negative, suggesting that glomerular injury was not associated with immune complex deposition (data not shown). Damaged glomeruli were distributed evenly in renal superficial cortex as well as in the juxtaglomerular area. Hyalinosis of arterioles (Figure 2I) or the vascular pole of the glomerulus (Figure 2L) rarely was observed in diabetic eNOS KO mice. It is interesting that arteriolar hyalinosis, when present, often was associated with glomerular mesangiolysis (Figure 2I). Mesangiolysis also correlated with blood glucose levels in diabetic eNOS KO mice (Figure 3B), whereas nondiabetic eNOS KO mice rarely developed mesangiolysis at 5 mo (Table 4). In addition, insulin treatment blocked the development of mesangial expansion, mesangiolysis, and the development of the nodular lesions at 3 and 5 mo (Tables 2 and 4).

Nondiabetic eNOS KO mice also demonstrated rare focal areas of tubular atrophy with condensed, hypoplastic glomeruli (Figure 4F). In these areas, the arterioles were severely constricted or occluded (Figure 4G). Low-grade mesangiolysis also was observed in nondiabetic eNOS KO mice at 5 mo (Table 4).

Glomerular Ultrastructure

Electron microscopic examination demonstrated no ultrastructural abnormalities in glomerulus in nondiabetic eNOS KO mice (Figure 5, A and B). However, diabetic eNOS KO mice developed markedly expanded mesangium with extracellular matrix and mesangial cell processes, thickened lamina densa, and subendothelial space (Figure 5, C and D). Glomerular capillary contained morphologically activated endothelial cell with enlarged nucleus (Figure 5E). Fibrin deposit also was attached on glomerular endothelial cells (Figure 5F). GBM width was increased in diabetic eNOS KO mice compared with nondiabetic eNOS KO mice (200 ± 28 *versus* 169 ± 20 μm, diabetic *versus* nondiabetic eNOS KO; $P < 0.05$; Figure 3). The

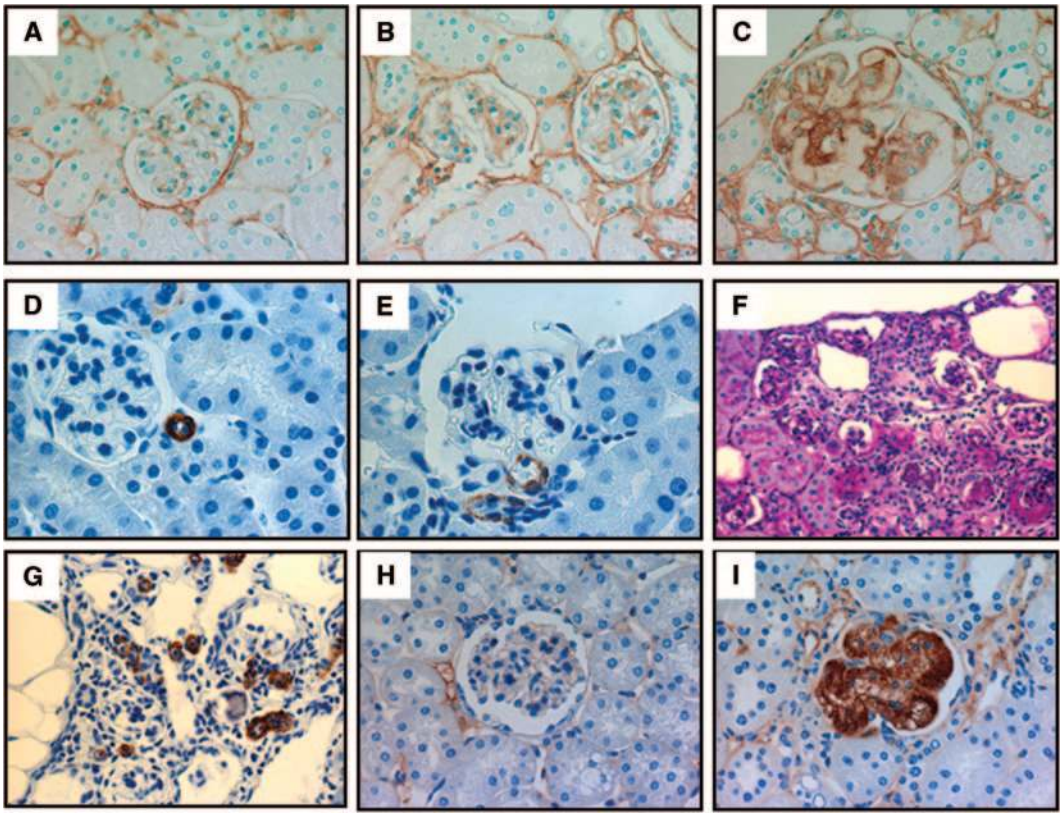

Figure 4. Histologic renal lesions in DM eNOS KO mouse. (A) Immunohistochemistry for glomerular collagen IV deposition in C57BL6 at 5 mo. (B) Collagen IV deposition in DM C57BL6 mouse at 5 mo. (C) Collagen IV in DM eNOS KO mouse at 5 mo. (D) Immunohistochemistry for smooth muscle actin (SMA) in afferent arteriole in non-DM C57BL6 at 3 mo. Brown color indicates SMA staining. (E) Immunohistochemistry for SMA (brown color) in arteriole in DM eNOS KO. Arteriole in DM eNOS KO mouse is dilated compared with that in non-DM C57BL6 at 3 mo. (F) PAS staining in non-DM eNOS KO mouse. Atubular glomeruli are observed rarely in cortex. (G) Immunohistochemistry for SMA (brown color) in non-DM eNOS KO mouse. Constricted or occluded arterioles are observed along with atubular glomeruli in non-DM eNOS KO mouse. (H) Immunohistochemistry for fibrin (brown color) in DM-C57BL6 mouse. (I) Fibrin staining (brown color) in DM eNOS KO mouse. Magnifications: ×400 in A, B, C, F, and G; ×1000 in D and E; ×630 in H and I.

Table 3. Glomeruli with fibrin deposition

Parameter	5 Mo (%)		
	Control	DM	DMIns
C57BL6	0	0	0
eNOS KO	1.8 ± 0.7	17.4 ± 2.9[a]	5.4 ± 6.1

[a] $P < 0.01$ *versus* non-DM, DMIns.

expanded mesangium revealed clusters of mesangial matrix microfibrils (Figure 6C) as well as mesangial cell processes with smaller intracellular microfilament bundles (Figure 6D) inserting into membrane complexes.

Renal Arteriolar Histology

We previously demonstrated in other models that the development of preglomerular arteriolar disease results in altered autoregulation and can predispose kidneys to progression (28). We also showed that preglomerular arteriolar disease occurs with blockade of NO synthesis with L-NAME (29). We therefore examined the morphology of the afferent arteriole in both diabetic and nondiabetic mice. As shown in Figure 6, the lumens of arterioles of eNOS KO mice were larger than those observed in C57BL6 mice. In mice with diabetes there was a further increase in the inner lumen size in eNOS KO mice compared with nondiabetic C57BL6 mice (Figure 4, D and E). This increase was blocked by insulin treatment (Figure 7A). Conversely, the total vascular smooth muscle wall area was not different in these mice (Figure 7C). It is interesting that glomeruli with mesangiolysis were significantly associated with dilated arterioles (Figure 7B) as well as an increase in vascular smooth muscle wall area (Figure 7D) compared with glomeruli without mesangiolysis.

Angiogenesis (Endothelial Cell Proliferation)

VEGF mRNA expression was increased in diabetic C57BL6 and eNOS KO mice (Figure 8D). Importantly, insulin treatment blocked this upregulation of VEGF, demonstrating a key role

Table 4. Glomeruli with mesangiolysis

Parameter	3 Mo (%)			5 Mo (%)		
	Control	DM	DMIns	Control	DM	DMIns
C57BL6	0	0	0	0	0	0
eNOS KO	0	7.4 ± 2.1[a]	0.3 ± 0.5	1.2 ± 0.7	10.4 ± 5.6[a]	3.6 ± 1.2

[a] $P < 0.01$ *versus* non-DM, DMIns.

for glucose in regulating VEGF regardless of the status of the eNO system.

Endothelial morphology was assessed by immunostaining for CD34 (22) and thrombomodulin (21). Both diabetic eNOS KO and C57BL6 mice showed a generalized increase in endothelial cells in the cortex as noted by immunostaining for either CD34 or thrombomodulin (Figures 8 and 9), and this was associated with enhanced endothelial cell proliferation, as noted by double staining with Ki-67 and thrombomodulin or CD34 (Figure 9, G and H). Both endothelial proliferation and endothelial immunostaining were increased in eNOS diabetic KO compared with diabetic C57BL6 mice (Figure 8, A through C). Insulin treatment also largely corrected the increase in endothelial cell proliferation and number. In contrast, focal loss of endothelial cell staining was observed occasionally, particularly in glomeruli that displayed mesangiolysis (Figure 9, A and B).

Discussion

In this study, we present a mouse model of diabetic kidney disease that closely resembles human diabetic nephropathy. Diabetic mice that lacked the eNOS gene demonstrated classic features of diabetic nephropathy with intrarenal vascular disease, mesangial expansion with mesangiolysis and occasional microaneurysm formation, and the development of mesangial nodular (Kimmelstiel-Wilson) lesions. These changes could be prevented largely by insulin. Collectively, the data strongly suggest that a relative deficiency in eNO levels may be one of the long-sought risk factors that are critical for the increased susceptibility for nephropathy in individuals with diabetes.

We identified two potential major mechanisms to account for why eNOS KO phenotype may predispose to the development of diabetic nephropathy. First, eNOS KO mice developed systemic hypertension and heterogeneous afferent arteriolar lesions. In collaboration with the late Jaime Herrera-Acosta, our group demonstrated that preglomerular arteriolar disease may predispose the animal to renal progression ("the Herrera hypothesis") (30). Heterogeneity of afferent arteriolar lesions was observed in eNOS KO mice and were increased in the presence of diabetes. This heterogeneity of arteriolar lesions could result in some glomeruli being overperfused and others underperfused for the same renal arterial perfusion pressure. The association of mesangiolysis with dilated arteriole (Figure 7B) suggests that overperfusion in glomerulus could account for mesangial lesions (31,32). However, the underperfused glomeruli may become ischemic, leading to persistent stimulation of juxtaglomerular renin release, consistent with hypotheses on the mechanism for the development of essential hypertension (28,33). As a consequence, more severe systemic hypertension develops, which in turn acts in a vicious cycle to accelerate the glomerular hypertension and renal progression.

A second potential mechanism by which eNOS KO mice may be more susceptible to diabetic nephropathy is due to the dysregulation of the VEGF-NO axis (20). Normally, VEGF acts on endothelial cells largely *via* stimulation of eNOS (8). NO negatively regulates VEGF-induced endothelial cell proliferation, resulting in the maintenance of endothelial cell integrity (20). However, when endothelial NO levels are low, an increase in VEGF expression is associated with a marked NO-independent endothelial proliferative response (19,20). We have found that elevated glucose can cause this uncoupling *in vitro* (20).

Consistent with the uncoupling hypothesis was our observation that endothelial cell staining and proliferation were increased in diabetic eNOS KO mice compared with diabetic control mice. Importantly, the increased expression of VEGF was blocked in both groups of mice with insulin treatment. This demonstrates that the regulation of VEGF expression seems to depend primarily on glucose levels as opposed to eNO levels in this model. In addition, the observation that endothelial staining was greater in eNOS KO mice compared with C57BL6 mice regardless of presence of diabetes suggests the importance of the uncoupling hypothesis in augmenting the endothelial proliferative response (20). In contrast, Murohara *et al.* (34) reported that eNOS KO mice exhibited impaired angiogenesis in the hind limb ischemic model. In their model, however, the ischemic insult failed to increase VEGF expression, whereas, in our model, the primary stimulus for VEGF expression seemed to be hyperglycemia.

Whereas endothelial cell density and proliferation were increased overall in diabetic eNOS KO mice compared with diabetic C57BL6 mice, the diabetic eNOS KO mice also showed focal areas of capillary loss and evidence of endothelial injury as noted by the intracapillary fibrin staining. It is interesting that the presence of mesangiolysis was associated with loss of glomerular endothelial cells, whereas most other glomeruli showed an endothelial proliferative response in diabetic eNOS KO mice. This heterogeneity of endothelial response could be associated with the heterogeneity of mesangial cell proliferation. Indeed, it has been demonstrated that a glomerulus simultaneously exhibits mesangial proliferation and mesangiolysis in human diabetic nephropathy (3). Furthermore, it is compatible with the evidence that anti–Thy1-induced mesangiolysis in rat is associated with loss of both mesangial and endothelial cells

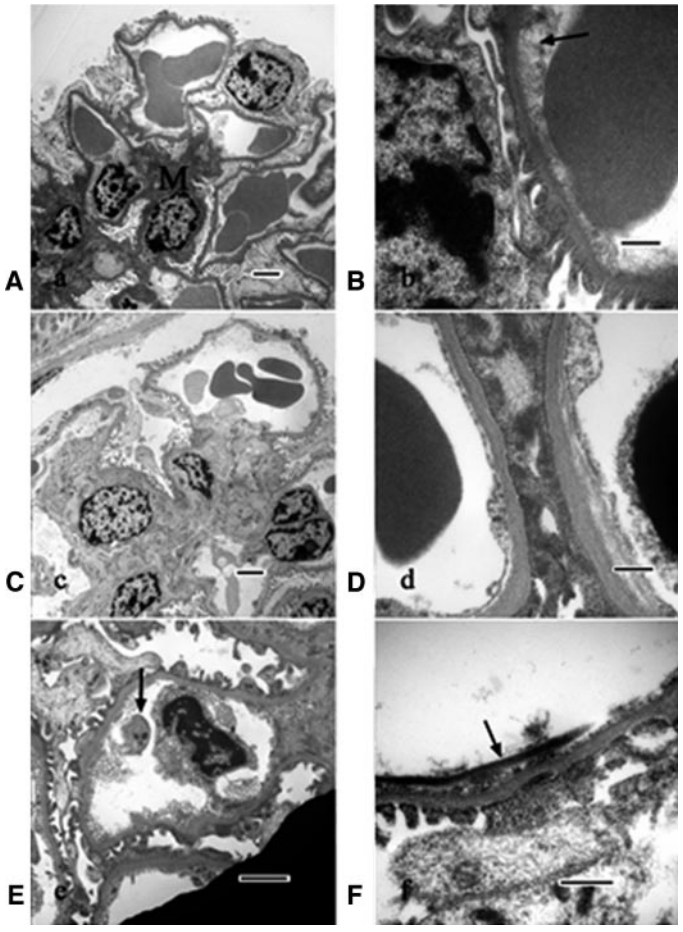

Figure 5. Ultrastructural histology in non-DM and DM eNOS KO mice. (A) Lower magnification of non-DM eNOS kidney showing mesangium (M) surrounded by capillaries with red blood cells (RBC). Endothelium is not apparent at this magnification (bar = 2 μm). (B) Higher magnification of non-DM eNOS KO kidney with RBC in capillary lumen (top far right), preserved endothelial cells (arrow), basement membrane (center,) and podocyte with foot processes (in center and far left). Representative basement membrane used for width measurement (bar = 500 nm). (C) DM eNOS KO kidney with markedly expanded mesangium (center) at same magnification as A. (D) Higher magnification of DM eNOS KO kidney with thickened lamina densa (see text) and subendothelial space (bar = 500 nm). Representative area used for measurement. (E) DM eNOS KO glomerular capillary with morphologically activated, partially elevated endothelial cell with enlarged nucleus, markedly ruffled cell membrane, and marginated platelet (arrow; bar = 2 μm). (F) Higher magnification of DM capillary wall with attached fibrin deposit (arrow) and partially degenerated endothelial cell in DM eNOS KO mouse (bar = 500 nm).

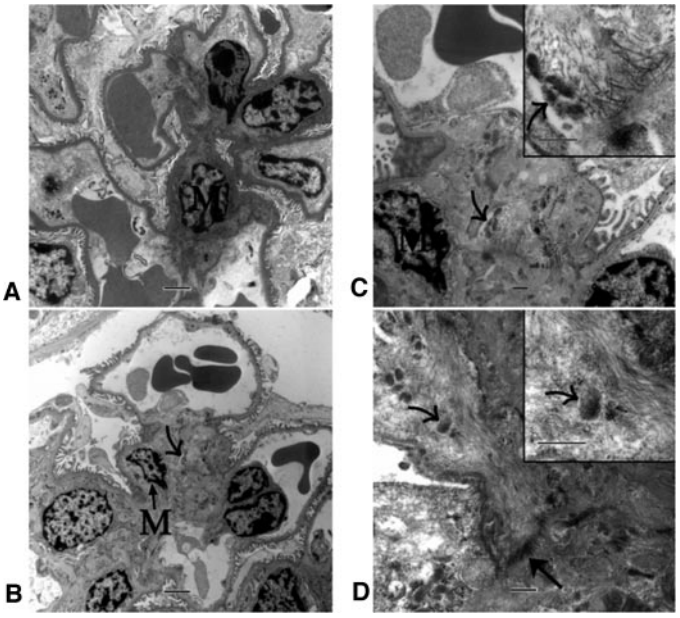

Figure 6. The fibrillar mesangial expansion in DM eNOS KO mouse. (A) Low-magnification view of non-DM eNOS KO mouse showing normal structure of peripheral capillary lobule. A mesangial nucleus is noted (M). Bar = 2.0 μm. (B) View of peripheral capillary lobule in DM eNOS KO mouse at same magnification as A. Bowman's capsule is seen at top left. A mesangial cell nucleus (M) is marked with straight arrow. Mesangial expansion is evident and confirms the light microscopic appearance with cell processes and matrix expansion. The areas marked with curved arrow are shown at higher magnification in C. Bar = 2.0 μm. (C) Higher power view of B with the same mesangial cell nucleus (M). The region near the curved arrow is shown at higher power in the inset. A cluster of mesangial matrix microfibrils of approximately 15-nm (10 to 20 nm) diameter are present to the right of the arrow. Bar = 500 nm in each part. (D) A mesangial cell cytoplasmic process with attachment to the matrix (straight arrow). The region of the curved arrow is shown at the same higher magnification (as inset) to demonstrate clearly the smaller intracellular microfilament bundles (7-nm diameter). Bar = 500 nm in each part.

followed by both mesangial and glomerular endothelial cell proliferation (35).

Currently, endothelial dysfunction is considered a component of mesangiolysis that is associated with thrombotic microangiopathy (36). Although the precise mechanism has not been clarified yet, detached endothelial cells or widening of the subendothelial space is associated with mesangiolysis in diabetes and other diseases, such as cyclosporine nephropathy or transplant glomerulopathy (36,37). We postulate that endothelial dysfunction as a result of targeted deletion of eNOS gene could be a mechanism for mesangiolysis in this model. It is interesting that nondiabetic eNOS KO mice also developed mild glomerular lesions at 5 mo, suggesting that endothelial dysfunction as a result of deletion of the eNOS gene could cause mesangiolysis directly or indirectly (Table 4). However, the marked increase in renal injury (including systemic hypertension, mesangiolysis, and nodule formation) in diabetic eNOS KO mice and the reversal with insulin strongly suggest an eNO and glucose interaction. A strong relationship between endothelial dysfunction and diabetic nephropathy in humans also has been noted (38), consistent with such an interaction. Importantly, this model is distinct from simply inducing diabetes in hypertensive animals, such as spontaneous hypertensive rat

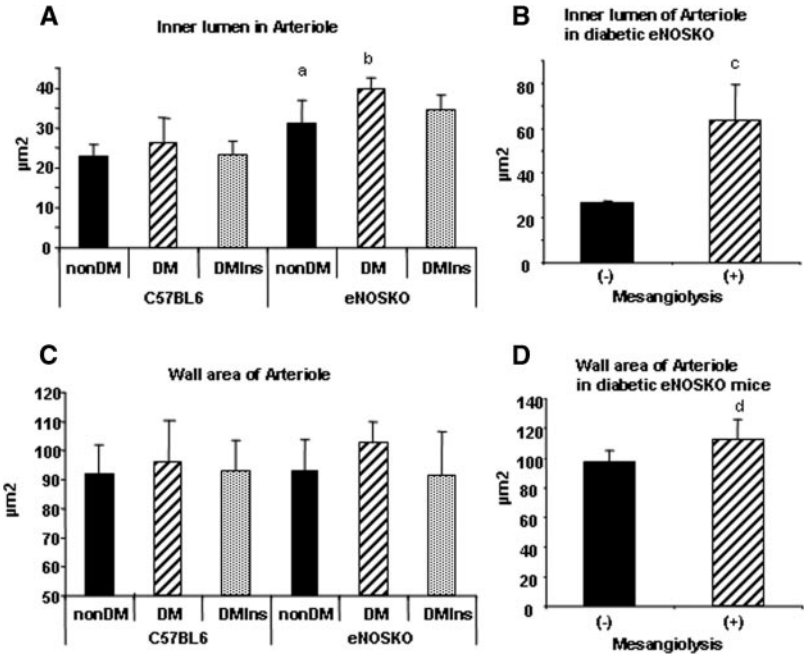

Figure 7. (A) Inner lumen size in afferent arteriole. [a]$P < 0.01$ *versus* C57BL6; [b]$P < 0.05$ *versus* non-DM in eNOS KO mice. (B) Inner lumen of afferent arteriole in DM eNOS KO mice. Glomerulus with mesangiolysis is associated with dilated arteriole. (C) Wall area of afferent arteriole. (D) Wall area of arteriole in DM eNOS KO mice.

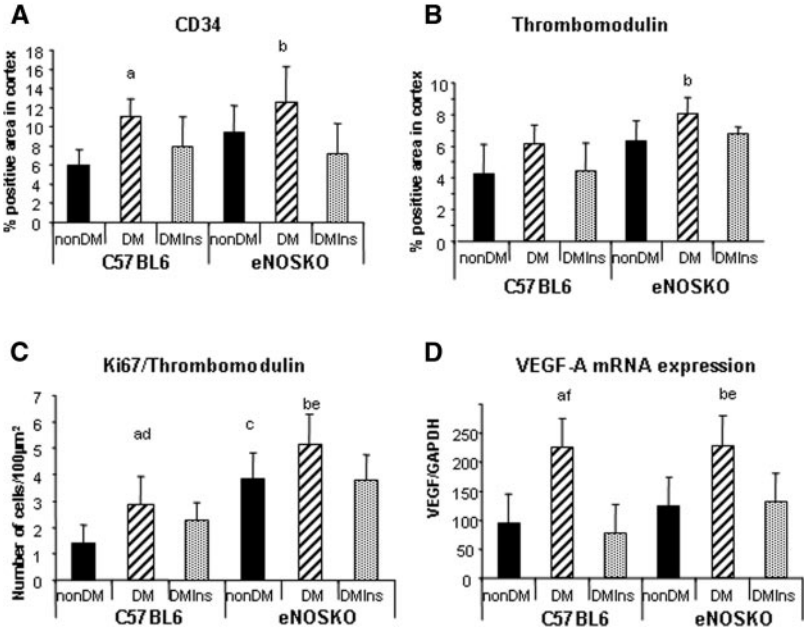

Figure 8. (A) Quantification of CD34 in cortex. (B) Quantification of TM staining. (C) Cell number with double staining for TM and Ki-67 in renal cortex per 100 μm^2. (D) Real-time PCR for vascular endothelial growth factor (VEGF) mRNA expression in whole kidney at 3 mo. [a]$P < 0.05$ *versus* non-DM in C57BL6; [b]$P < 0.05$ *versus* DMIns in eNOS KO; [c]$P < 0.05$ *versus* non-DM in C57BL6; [d]$P < 0.05$ *versus* DM in eNOS KO; [e]$P < 0.05$ *versus* nonDM in eNOS KO.

and hypertensive transgenic mREN2–27 rat, and it is interesting that these animals do not develop mesangiolysis under diabetic conditions (39,40). This suggests that hypertension *per se* is unlikely to induce mesangiolysis unless the autoregulatory mechanisms are altered.

In this model, we also observed evidence of endothelial injury, and this was associated with fibrin deposition and mesangiolysis. These lesions also are observed in thrombotic microangiopathies, raising the possibility that this model is not a pure model of diabetic nephropathy. Indeed, fibrin and mesan-

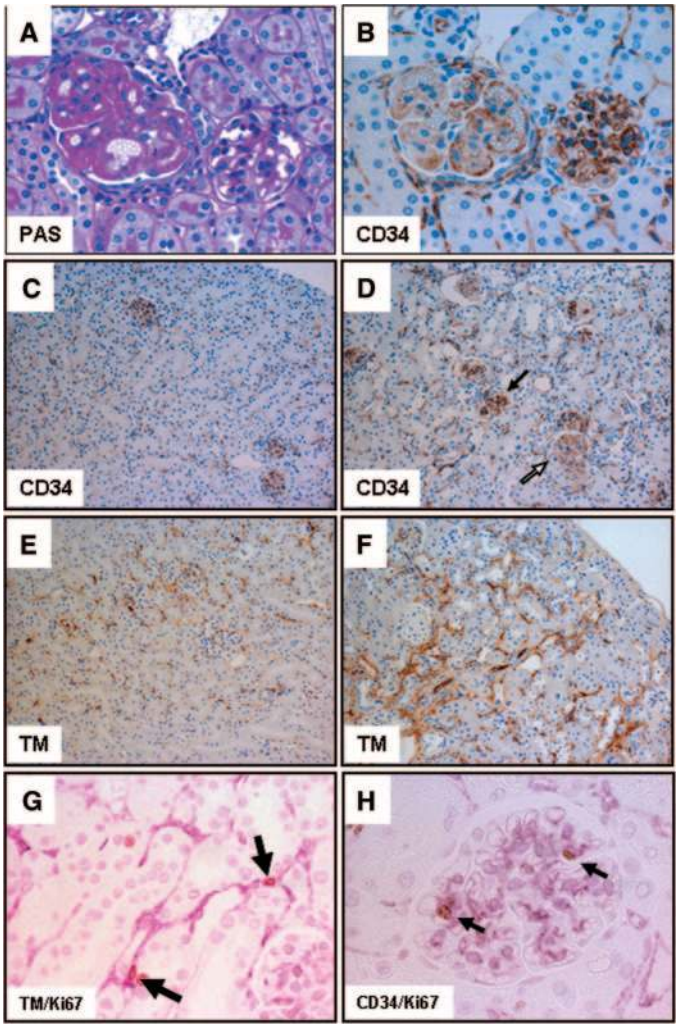

Figure 9. Endothelial cell proliferation in DM eNOS KO mouse. (A) PAS staining of injured glomerulus in DM eNOS KO mouse at 3 mo. (B) Immunostaining for CD34. Brown color indicates CD34 staining as a marker of endothelial cell. Blue color indicates counterstaining for nucleus with hematoxylin. Loss of endothelial cell is observed in injured glomerulus in DM eNOS KO mouse at 3 mo. (C) Immunohistochemistry for CD34 in non-DM C57BL6. (D) CD34 in DM eNOS KO kidney. Some glomeruli show strong immunoreactivity (block arrow), whereas some show less endothelial staining (white arrow). (E) Immunostaining for thrombomodulin (TM) (brown color) in non-DM C57BL6. TM is expressed primarily in peritubular capillary. (F) TM in DM eNOS KO. TM staining is heavier than that in C. (G) Double staining for TM (Bjoran Purple; white arrow) and Ki-67 (dark brown). Double staining can indicate proliferating endothelial cell (arrow). (H) Proliferating endothelial cell detected (arrow) by double staining of glomerular capillary for TM (purple) and Ki-67 (dark brown). Original magnifications: ×630 in A, B, G, and H; ×200 in C through F.

giolysis were observed less commonly in some recent pathologic studies of diabetic nephropathy (3). However, in the older literature, numerous studies demonstrated the activation of intrarenal coagulation as well as fibrin deposition (41,42) in association with mesangiolysis and mesangial nodule formation (42). We believe that this was observed more commonly in the past, before the use of effective antihypertensive agents and better blood sugar control.

We suggest that this new murine model of diabetic nephropathy may be relevant to human diabetic disease. This experimental model supports the interpretation of human pathology and the hypothesis that there are three histologic appearances of glomeruli in diabetes: Diffuse intercapillary glomerulosclerosis; nodular intercapillary glomerulosclerosis; and a third progressive lesion of mesangiolysis, capillary microaneurysms and nodular scarring. In addition to the similar histologic findings, human diabetic nephropathy is strongly associated with endothelial dysfunction, likely a consequence of the effects of glucose (43), advance glycation end products (44), uric acid (45), C-reactive protein (46), oxidative stress (47), and asymmetric dimethylarginine (48) to reduce eNO bioavailability. The relatively lower levels of uric acid and asymmetric dimethylarginine in mice could provide a potential explanation for why rodents are less likely to develop classic diabetic renal disease. Furthermore, the importance of the eNOS gene in the development of diabetic nephropathy and retinopathy was recognized recently (49). In particular, the polymorphism T-786C is associated with both nephropathy and retinopathy (49).

Conclusion

It is widely known that only 30 to 40% of individuals with type 1 diabetes will develop significant nephropathy. On the basis of the findings in this article, we propose that it is the level of eNO that may be one of the critical determinants for whether patients with diabetes are at risk for developing nephropathy. Because endothelial function can be assessed readily by measurements such as brachial artery reactivity, we believe that clinical studies to address this hypothesis are feasible.

Acknowledgments

This study was supported by a Program Project from the Juvenile Diabetes Research Foundation and by generous funds from Gatorade. T.N. and R.J.J. also are supported by National Institutes of Health grants DK-52121 and HL-68607.

Disclosures

R.J.J. is a consultant for Scios Inc., TAP Pharmaceuticals, and Nephromics Inc.

References

1. Breyer MD, Bottinger E, Brosius FC 3rd, Coffman TM, Harris RC, Heilig CW, Sharma K: Mouse models of diabetic nephropathy. *J Am Soc Nephrol* 16: 27–45, 2005
2. Saito Y, Kida H, Takeda S, Yoshimura M, Yokoyama H, Koshino Y, Hattori N: Mesangiolysis in diabetic glomeruli: Its role in the formation of nodular lesions. *Kidney Int* 34: 389–396, 1988
3. Stout LC, Kumar S, Whorton EB: Focal mesangiolysis and the pathogenesis of the Kimmelstiel-Wilson nodule. *Hum Pathol* 24: 77–89, 1993

4. Min W, Yamanaka N: Three-dimensional analysis of increased vasculature around the glomerular vascular pole in diabetic nephropathy. *Virchows Arch A Pathol Anat Histopathol* 423: 201–207, 1993
5. Kanesaki Y, Suzuki D, Uehara G, Toyoda M, Katoh T, Sakai H, Watanabe T: Vascular endothelial growth factor gene expression is correlated with glomerular neovascularization in human diabetic nephropathy. *Am J Kidney Dis* 45: 288–294, 2005
6. de Vriese AS, Tilton RG, Elger M, Stephan CC, Kriz W, Lameire NH: Antibodies against vascular endothelial growth factor improve early renal dysfunction in experimental diabetes. *J Am Soc Nephrol* 12: 993–1000, 2001
7. Flyvbjerg A, Dagnaes-Hansen F, De Vriese AS, Schrijvers BF, Tilton RG, Rasch R: Amelioration of long-term renal changes in obese type 2 diabetic mice by a neutralizing vascular endothelial growth factor antibody. *Diabetes* 51: 3090–3094, 2002
8. Ziche M, Morbidelli L, Choudhuri R, Zhang HT, Donnini S, Granger HJ, Bicknell R: Nitric oxide synthase lies downstream from vascular endothelial growth factor-induced but not basic fibroblast growth factor-induced angiogenesis. *J Clin Invest* 99: 2625–2634, 1997
9. Masuda Y, Shimizu A, Mori T, Ishiwata T, Kitamura H, Ohashi R, Ishizaki M, Asano G, Sugisaki Y, Yamanaka N: Vascular endothelial growth factor enhances glomerular capillary repair and accelerates resolution of experimentally induced glomerulonephritis. *Am J Pathol* 159: 599–608, 2001
10. Brodsky SV, Gao S, Li H, Goligorsky MS: Hyperglycemic switch from mitochondrial nitric oxide to superoxide production in endothelial cells. *Am J Physiol Heart Circ Physiol* 283: H2130–H2139, 2002
11. Du XL, Edelstein D, Dimmeler S, Ju Q, Sui C, Brownlee M: Hyperglycemia inhibits endothelial nitric oxide synthase activity by posttranslational modification at the Akt site. *J Clin Invest* 108: 1341–1348, 2001
12. Da Silva-Azevedo L, Baum O, Zakrzewicz A, Pries AR: Vascular endothelial growth factor is expressed in endothelial cells isolated from skeletal muscles of nitric oxide synthase knockout mice during prazosin-induced angiogenesis. *Biochem Biophys Res Commun* 297: 1270–1276, 2002
13. Bussolati B, Dunk C, Grohman M, Kontos CD, Mason J, Ahmed A: Vascular endothelial growth factor receptor-1 modulates vascular endothelial growth factor-mediated angiogenesis via nitric oxide. *Am J Pathol* 159: 993–1008, 2001
14. Couper LL, Bryant SR, Eldrup-Jorgensen J, Bredenberg CE, Lindner V: Vascular endothelial growth factor increases the mitogenic response to fibroblast growth factor-2 in vascular smooth muscle cells in vivo via expression of fms-like tyrosine kinase-1. *Circ Res* 81: 932–939, 1997
15. Grosskreutz CL, Anand-Apte B, Duplaa C, Quinn TP, Terman BI, Zetter B, D'Amore PA: Vascular endothelial growth factor-induced migration of vascular smooth muscle cells in vitro. *Microvasc Res* 58: 128–136, 1999
16. Parenti A, Bellik L, Brogelli L, Filippi S, Ledda F: Endogenous VEGF-A is responsible for mitogenic effects of MCP-1 on vascular smooth muscle cells. *Am J Physiol Heart Circ Physiol* 286: H1978–1984, 2004
17. Wang H, Keiser JA: Vascular endothelial growth factor upregulates the expression of matrix metalloproteinases in vascular smooth muscle cells: Role of flt-1. *Circ Res* 83: 832–840, 1998
18. Kang D, Nakagawa T, Feng L, Johnson RJ: Nitric oxide modulates vascular disease in the remnant kidney model. *Am J Pathol* 161: 239–248, 2002
19. Zhao Q, Egashira K, Inoue S, Usui M, Kitamoto S, Ni W, Ishibashi M, Hiasa Ki K, Ichiki T, Shibuya M, Takeshita A: Vascular endothelial growth factor is necessary in the development of arteriosclerosis by recruiting/activating monocytes in a rat model of long-term inhibition of nitric oxide synthesis. *Circulation* 105: 1110–1115, 2002
20. Nakagawa T, Sato W, Sautin YY, Glushakova O, Croker B, Atkinson MA, Tisher CC, Johnson RJ: Uncoupling of vascular endothelial growth factor with nitric oxide as a mechanism for diabetic vasculopathy. *J Am Soc Nephrol* 17: 736–745, 2006
21. Yuzawa Y, Brentjens JR, Brett J, Caldwell PR, Esposito C, Fukatsu A, Godman G, Stern D, Andres G: Antibody-mediated redistribution and shedding of endothelial antigens in the rabbit. *J Immunol* 150: 5633–5646, 1993
22. Fina L, Molgaard HV, Robertson D, Bradley NJ, Monaghan P, Delia D, Sutherland DR, Baker MA, Greaves MF: Expression of the CD34 gene in vascular endothelial cells. *Blood* 75: 2417–2426, 1990
23. Jensen EB, Gundersen HJ, Osterby R: Determination of membrane thickness distribution from orthogonal intercepts. *J Microsc* 115: 19–33, 1979
24. Kosugi T, Yuzawa Y, Sato W, Kawai H, Matsuo S, Takei Y, Muramatsu T, Kadomatsu K: Growth factor midkine is involved in the pathogenesis of diabetic nephropathy. *Am J Pathol* 168: 9–19, 2006
25. Mazzali M, Kanellis J, Han L, Feng L, Xia YY, Chen Q, Kang DH, Gordon KL, Watanabe S, Nakagawa T, Lan HY, Johnson RJ: Hyperuricemia induces a primary renal arteriolopathy in rats by a blood pressure-independent mechanism. *Am J Physiol Renal Physiol* 282: F991–F997, 2002
26. Nakagawa T, Lan HY, Zhu HJ, Kang DH, Schreiner GF, Johnson RJ: Differential regulation of VEGF by TGF-beta and hypoxia in rat proximal tubular cells. *Am J Physiol Renal Physiol* 287: F658–F664, 2004
27. Emanueli C, Salis MB, Van Linthout S, Meloni M, Desortes E, Silvestre JS, Clergue M, Figueroa CD, Gadau S, Condorelli G, Madeddu P: Akt/protein kinase B and endothelial nitric oxide synthase mediate muscular neovascularization induced by tissue kallikrein gene transfer. *Circulation* 110: 1638–1644, 2004
28. Johnson RJ, Feig DI, Herrera-Acosta J, Kang DH: Resurrection of uric acid as a causal risk factor in essential hypertension. *Hypertension* 45: 18–20, 2005
29. Quiroz Y, Pons H, Gordon KL, Rincon J, Chavez M, Parra G, Herrera-Acosta J, Gomez-Garre D, Largo R, Egido J, Johnson RJ, Rodriguez-Iturbe B: Mycophenolate mofetil prevents salt-sensitive hypertension resulting from nitric oxide synthesis inhibition. *Am J Physiol Renal Physiol* 281: F38–F47, 2001
30. Sanchez-Lozada LG, Tapia E, Santamaria J, Avila-Casado C, Soto V, Nepomuceno T, Rodriguez-Iturbe B, Johnson RJ, Herrera-Acosta J: Mild hyperuricemia induces vasoconstriction and maintains glomerular hypertension in normal and remnant kidney rats. *Kidney Int* 67: 237–247, 2005
31. Wang X, Aukland K, Bostad L, Iversen BM: Autoregulation of total and zonal glomerular filtration rate in spontane-

ously hypertensive rats with mesangiolysis. *Kidney Blood Press Res* 20: 11–17, 1997
32. Hartner A, Cordasic N, Klanke B, Muller U, Sterzel RB, Hilgers KF: The alpha8 integrin chain affords mechanical stability to the glomerular capillary tuft in hypertensive glomerular disease. *Am J Pathol* 160: 861–867, 2002
33. Sealey JE, Blumenfeld JD, Bell GM, Pecker MS, Sommers SC, Laragh JH: On the renal basis for essential hypertension: Nephron heterogeneity with discordant renin secretion and sodium excretion causing a hypertensive vasoconstriction-volume relationship. *J Hypertens* 6: 763–777, 1988
34. Murohara T, Asahara T, Silver M, Bauters C, Masuda H, Kalka C, Kearney M, Chen D, Symes JF, Fishman MC, Huang PL, Isner JM: Nitric oxide synthase modulates angiogenesis in response to tissue ischemia. *J Clin Invest* 101: 2567–2578, 1998
35. Iruela-Arispe L, Gordon K, Hugo C, Duijvestijn AM, Claffey KP, Reilly M, Couser WG, Alpers CE, Johnson RJ: Participation of glomerular endothelial cells in the capillary repair of glomerulonephritis. *Am J Pathol* 147: 1715–1727, 1995
36. Morita T, Yamamoto T, Churg J: Mesangiolysis: An update. *Am J Kidney Dis* 31: 559–573, 1998
37. Leontsini M: Mesangiolysis. *Hippokratia* 7: 147–151, 2003
38. Jawa A, Nachimuthu S, Pendergrass M, Asnani S, Fonseca V: Impaired vascular reactivity in African-American patients with type 2 diabetes mellitus and microalbuminuria or proteinuria despite angiotensin-converting enzyme inhibitor therapy. *J Clin Endocrinol Metab* 91: 31–35, 2006
39. Cooper ME, Allen TJ, O'Brien RC, Macmillan PA, Clarke B, Jerums G, Doyle AE: Effects of genetic hypertension on diabetic nephropathy in the rat: Functional and structural characteristics. *J Hypertens* 6: 1009–1016, 1988
40. Kelly DJ, Wilkinson-Berka JL, Allen TJ, Cooper ME, Skinner SL: A new model of diabetic nephropathy with progressive renal impairment in the transgenic (mRen-2)27 rat (TGR). *Kidney Int* 54: 343–352, 1998
41. Farquhar A, MacDonald MK, Ireland JT: The role of fibrin deposition in diabetic glomerulosclerosis: A light, electron and immunofluorescence microscopy study. *J Clin Pathol* 25: 657–667, 1972
42. Stout LC, Kumar S, Whorton EB: Insudative lesions: Their pathogenesis and association with glomerular obsolescence in diabetes—A dynamic hypothesis based on single views of advancing human diabetic nephropathy. *Hum Pathol* 25: 1213–1227, 1994
43. Title LM, Cummings PM, Giddens K, Nassar BA: Oral glucose loading acutely attenuates endothelium-dependent vasodilation in healthy adults without diabetes: An effect prevented by vitamins C and E. *J Am Coll Cardiol* 36: 2185–2191, 2000
44. Tan KC, Chow WS, Ai VH, Metz C, Bucala R, Lam KS: Advanced glycation end products and endothelial dysfunction in type 2 diabetes. *Diabetes Care* 25: 1055–1059, 2002
45. Bo S, Cavallo-Perin P, Gentile L, Repetti E, Pagano G: Hypouricemia and hyperuricemia in type 2 diabetes: Two different phenotypes. *Eur J Clin Invest* 31: 318–321, 2001
46. Tan KC, Chow WS, Tam SC, Ai VH, Lam CH, Lam KS: Atorvastatin lowers C-reactive protein and improves endothelium-dependent vasodilation in type 2 diabetes mellitus. *J Clin Endocrinol Metab* 87: 563–568, 2002
47. Beckman JA, Goldfine AB, Gordon MB, Garrett LA, Keaney JF Jr, Creager MA: Oral antioxidant therapy improves endothelial function in type 1 but not type 2 diabetes mellitus. *Am J Physiol Heart Circ Physiol* 285: H2392–H2398, 2003
48. Tarnow L, Hovind P, Teerlink T, Stehouwer CD, Parving HH: Elevated plasma asymmetric dimethylarginine as a marker of cardiovascular morbidity in early diabetic nephropathy in type 1 diabetes. *Diabetes Care* 27: 765–769, 2004
49. Awata T, Neda T, Iizuka H, Kurihara S, Ohkubo T, Takata N, Osaki M, Watanabe M, Nakashima Y, Sawa T, Inukai K, Inoue I, Shibuya M, Mori K, Yoneya S, Katayama S: Endothelial nitric oxide synthase gene is associated with diabetic macular edema in type 2 diabetes. *Diabetes Care* 27: 2184–2190, 2004

See the related editorial, "Toward a Mouse Model of Diabetic Nephropathy: Is Endothelial Nitric Oxide Synthase the Missing Link?" on pages 364–366.